SIMULATION OF SEMICONDUCTOR PROCESSES AND DEVICES Vol. 12
Edited by T. Grasser and S. Selberherr - September 2007

Study of the Junction Depth Effect on Ballistic Current Using the Subband Decomposition Method

M. Ali. Pourghaderi*¶, Wim Magnus°, Bart Sorée*, Marc Meuris*, Marc Heyns*¶ and Kristin De Meyer*¶

* IMEC. Kapeldreef 75, B-3001, Leuven, Belgium
{pourgham|magnus|soree|meuris|heyns|demeyer}@imec.be

° Universiteit Antwerpen, Physics Dept.
Groenenborgerlaan 171, B-2020 Antwerpen, Belgium

¶ Katholieke Universiteit Leuven, INSYS
Kasteelpark Arenberg 10, B-3001 Leuven, Belgium

Abstract

A robust algorithm to get the chemical potential of the particle reservoirs for the self consistent full 2D Schrödinger-Poisson solver is proposed. Using this algorithm we study the effect of junction depth on ballistic current. Simulation results show that shallow junctions come with much better on to off current ratio while it keeps the on-state transconductance at the same level as the deeper junction device.

1 Introduction

An efficient 2D Schrödinger-Poisson solver for modern MOS transistors becomes inevitable. When open boundary conditions are imposed, only a limited number of methods can be used. Among these methods, the subband decomposition method [1] or quantum transmitting boundary method [2] come with great advantages. In this method, the reservoir picture is used to calculate carrier injection from source and drain. In order to model also the accumulation in the lightly doped drain (LDD) regions for a transistor in the on-state, the transistor area covered by the simulation should at least partially include the source and drain regions. In this light the chemical potential in source and drain should be properly calculated. This calculation is crucial to correctly impose the Dirichlet boundary condition of the Poisson equation and to calculate ballistic current and carrier distribution.

2 Algorithm

In each iteration, the chemical potential of a reservoir is calculated by assuming a 1D potential profile at the edge of the active area which can only be justified when we extend the active area far enough from the gated region. Fig. 1 shows such a wide active area and the coordinate axes used in the equations. For the region with a 1D potential profile the integral of the charge density in the confinement direction should

be zero due to zero electric field in bulk and Gauss' law. This yields the equation to get the chemical potential at each junction.

$$\frac{d^2}{dz^2}u(x_{P0},z)=\frac{q}{\varepsilon_{Si}}\left(p(x_{P0},z,\mu_{P0})+N_d(x_{P0},z)-n(x_{P0},z,\mu_{P0},\mu_{P1})-N_a(x_{P0},z)\right) \quad (1)$$

$$\begin{cases}\int_0^\infty \left(p(x_{P0},z,\mu_{P0})+N_d(x_{P0},z)-n(x_{P0},z,\mu_{P0},\mu_{P1})-N_a(x_{P0},z)\right)dz=F_0(\mu_{P0},\mu_{P1})=0 & \text{(2.a)}\\ \int_0^\infty \left(p(x_{P1},z,\mu_{P1})+N_d(x_{P1},z)-n(x_{P1},z,\mu_{P0},\mu_{P1})-N_a(x_{P1},z)\right)dz=F_1(\mu_{P0},\mu_{P1})=0 & \text{(2.b)}\end{cases}$$

$$n(x,z,\mu_{P0},\mu_{P1})=2\sum_p\sum_{i_0}^{\infty}\int_0^{\infty}\left|\psi_{p,i_0,k_x}(x,z)\right|^2\left(\int_{-\infty}^{\infty}f_{FD}\left(E(p,i_0,k_x,k_y)-\mu_p\right)\frac{dk_y}{2\pi}\right)\frac{dk_x}{2\pi} \quad (3)$$

Eq. (1) is the Poisson equation at the edge of active area, x_{P0}, where it is connected to reservoir $P0$. Being derived from classical Fermi-Dirac statistics, the hole concentration $p(x_{P0},z,\mu_{P0})$ merely depends on the chemical potential of reservoir $P0$. The electron concentration $n(x_{P0},z,\mu_{P0},\mu_{P1})$ contains a contribution to the carrier distribution at x_{P0} due to injection from reservoir $P1$. As a result the electron distribution depends on the chemical potentials μ_{P0} and μ_{P1} of both reservoirs, which may be obtained form Eqs. (2a,b). Considering the injection from both reservoirs and all possible confinement modes and plane waves, we use Fermi-Dirac statistics to statistically average the quantum mechanical density operator as mentioned in Eq.(3). This gives the quantum mechanical electron distribution for any x and z. The labels P, i_0 and k_x respectively denote the reservoir index, the mode index and the plane wave number in the channel direction. Fixing x at x_{P0} we can calculate $n(x_{P0},z,\mu_{P0},\mu_{P1})$ in (2).

We have compared our method with two other methods that evaluate the electron distributions across the junction: the classical method and a semi classical one, relying on Boltzmann statistics but pinching off the electron density at the oxide interface. This comparison shows that the difference between the chemical potentials is in the order of *kT*. This is due to the shallow junction of the short device for which quantum effects can not be neglected.

In order to achieve fast and efficient convergence, we invoke a filter for the 2D potential during the above calculation for chemical potential. The main reason for this is to prevent artificial carrier fluctuations in the heavily doped region. To reach this goal, we designed the filter to yield relatively flat and 1D-like potential profiles in the outer half of the source and drain regions. By gradually removing this filter during iterations we obtain a realistic potential profile with 1D behavior at the edge of source and drain as was originally assumed. The only remaining question concerns the choice of a proper width for the active area. It shouldn't be too wide due to run time restrictions and on other hand it should be wide enough to reach 1D behavior at edge of the active area.

Fig. 2 shows the overall algorithm. Using the potential profile of a previous iteration, we solve the 2D Schrödinger equation for all possible excitations to obtain

$F_0(\mu_{P0},\mu_{P1})$ and $F_1(\mu_{P0},\mu_{P1})$ in Eqs. (2a,b). Solving the latter, we get the chemical potential of the junctions. Next, we solve the 2D Schrödinger equation again, but this time we use the chemical potentials calculated in the previous step to obtain the electron density through Eq.(3), yielding excellent and smooth convergence. Fig. 3 shows a typical electron distribution for the doping profile shown in Fig.4.

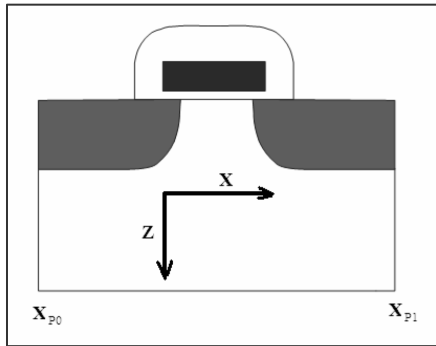

Figure 1: Simulation area with edges x_{P0} and x_{P1}.

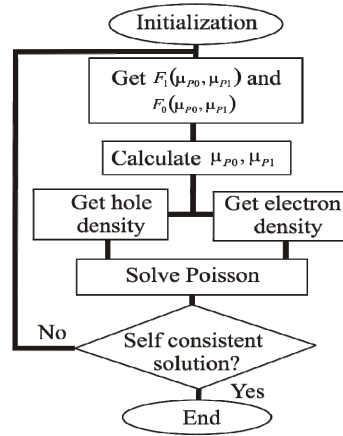

Figure 2: Flowchart of the algorithm

3 Simulation Results

We have simulated a traditional *n*-channel Si device with an electrical gate length of 10.2 nm. The gate length is 15 nm, but we account for a 2.4 nm overlap between the LDD and gated region. The doping profile in the LDD region is taken to be a 2D elliptical Gaussian profile with a base line of 5E19 cm^{-3}. The channel doping is 3.5E18 cm^{-3} and the oxide thickness is 1 nm. The junction depth is scanned from 6nm to 9nm. The ballistic current is calculated by statistical averaging of current density operator:

$$j(x,z)=2\sum_{p}\sum_{i_0}^{\infty}\int_{0}^{\infty}\frac{q\hbar}{m_x}\operatorname{Im}\left(\overline{\psi}_{p,i_0,k_x}(x,z)\nabla\psi_{p,i_0,k_x}(x,z)\right)\left(\int_{-\infty}^{\infty}f_{FD}\left(E(p,i_0,k_x,k_y)-\mu_p\right)\frac{dk_y}{2\pi}\right)\frac{dk_x}{2\pi} \quad (4)$$

Figs. 5 and 6 show that a reduction of the junction depth causes a lower on current and a much lower off current. A reduction of 1nm in junction depth suppresses the off current approximately by one order of magnitude. Fig. 5 shows that the transconductance is preserved down to7nm junction depth.

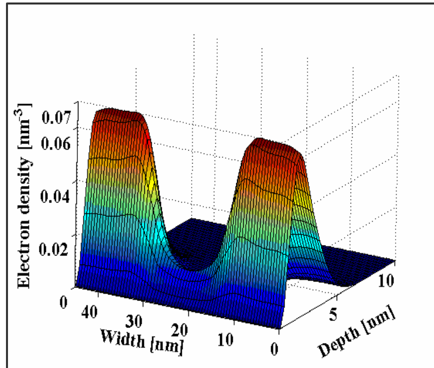

Figure 3: Electron density for Vgs = 0.4V ans V_{ds}=0V

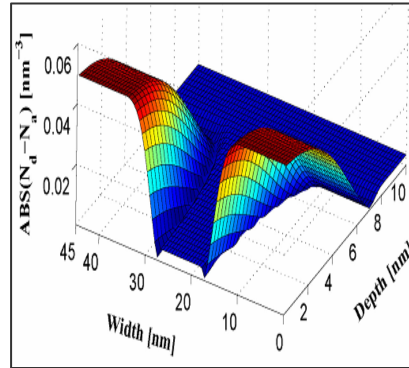

Figure 4: Doping concentration profile of simulated structure.

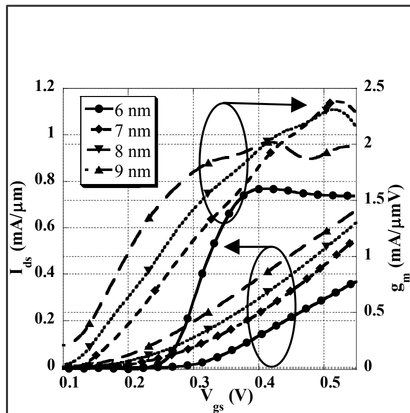

Figure 5: I_{ds} and g_m vs. V_{gs} for different junction depth. V_{ds} = 0.04 V.

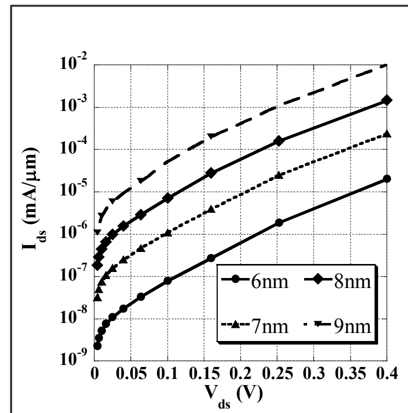

Figure 6: off current for different junction depth. V_{gs} is set to be zero.

4 Conclusion

A robust algorithm is presented for a 2D Schrödinger-Poisson solver with open boundary conditions and accounting for the junctions. It is shown that shallow junctions yield better on to off current ratio preserving the transconductance.

References

[1] E. Polizzi, N. Ben Abdallah, *Subband decomposition approach for the simulation of quantum electron transport in nanostructures*, Journal of Computational Physics **22**, 150-180 (2005).

[2] Craig S. Lent and David J. Kirkner, *The quantum transmitting boundary method*, Journal of Applied Physics **67**, 6353 (1990).